

Top decays into lighter stop and gluino

Shou Hua Zhu ^{a,b} and Lian You Shan ^b

a CCAST (World Lab), P.O. Box 8730, Beijing 100080, P.R. China

b Institute of Theoretical Physics, Academia Sinica, P.O. Box 2735, Beijing 100080, P.R. China

ABSTRACT

We have calculated the decay width of the process $t \rightarrow \tilde{g}\tilde{t}_1$ including one loop QCD corrections. We found that the QCD corrections could enhance the decay widths over 10% in a very large mass range of the lighter stop, and the decay width of the process could be larger than that of the channel $t \rightarrow bW^+$. Our results showed that such process, if allowed kinetically, must have very important phenomenology consequences; at least, new constrains for the masses of the lighter stop and gluino can be obtained.

PACS number: 14.65.Ha, 14.80.Ly

I. INTRODUCTION

The huge mass of the top quark arised from a large Yukawa coupling to the Higgs fields, as a supersymmetric counterpart, a large mass splitting can emerge between the mass-eigenstates of the stops and can lead to a lighter physical stop with a mass even smaller than that of the top quark [1]. Then the stop must contribute rich phenomena in the top quark factories (LHC et. al.).

The present colliders have given a mass bound heavier than 180 GeV for the gluino based on a controversial assumption that there is no gluino lighter than 5 GeV [2] or based on the state-of-art usage of perturbative theory [3]. However these experiments can never exclude the scenarios which favor a very light gluino [4].

The mass of gluino was resulted $1 \sim 100$ GeV typically if the SUSY breaking was transmitted to the observable sector by gravity (mSUDRA); the masses of gluinos and squarks will arise smaller as a loop interactions (next leading order effect) when that breaking is gauge-mediated (GMSB) [5]. These attractive GUT symmetric scenarios, which can explain several well-established phenomena, such as the $\eta(1410)$ [6] and anomalies in jet production [7]. With a light gluino, a noticeable partial width to stop and gluino may be detected in top quark decay when the statistics of the top events are improved. In fact, the standard model (SM) width $BR(t \rightarrow bW^+)$ had been assumed as the dominant one for the observed top pair events at Tevatron [8]. Thus, it is not excluded that the non-SM branching ratio of the top quark which could be as large as the SM one, and the searching for non-SM top decay are undergoing in both CDF and $D\emptyset$ [9].

Under the scenarios of the light gluino, Li et. al. [10] have studied the process $\tilde{g}\tilde{g} \rightarrow t\bar{t}$ at hadron colliders. In this paper, we will consider the decay process $t \rightarrow \tilde{g}\tilde{t}_1$ including the QCD corrections. In the literatures, There have been several works discussing the squarks and gluino decays with the same dynamics (interaction vertex) [11], such calculations offered a good reference to check our calculations.

II. CALCULATIONS

The tree level diagram of the process $t(p) \rightarrow \tilde{g}(k_1)\tilde{t}_1(k_2)$ is shown in Fig. 1 (a), and the decay width is

$$\Gamma_0 = \frac{N\alpha_s}{3m_t^3}(m_t^2 - m_{\tilde{g}}^2 + m_{\tilde{t}_1}^2 - 2m_{\tilde{g}}m_{\tilde{t}_1}\sin(2\theta)), \quad (1)$$

where

$$N = \sqrt{(m_t^2 - (m_{\tilde{g}} + m_{\tilde{t}_1})^2)(m_t^2 - (m_{\tilde{g}} - m_{\tilde{t}_1})^2)}, \quad (2)$$

and θ is the stop mixing angle which are defined in next section.

A. Virtual corrections

The $O(\alpha_s)$ virtual corrections arise from triangle as well as the gluino, quark and squark selfenergies diagrams as shown in Fig. 1 (b)-(e) respectively. Through our calculations, we employed dimensional reduction regularization (DRR) to control all the ultraviolet divergences, which is widely adopted in the calculations of the radiative corrections in the minimal supersymmetric standard model (MSSM) since the conventional dimensional regularization violates supersymmetry with a mismatch between the numbers of degree of freedom of gauge bosons and gauginos [12]. At the same time, we adopted the on-mass-shell renormalization scheme [13,14].

The one loop decay width can be expressed as

$$\begin{aligned} \Gamma_1 = & \frac{4\sqrt{2}\pi N\alpha_s^2}{3m_t^3} \operatorname{Re} \left(f_1((m_{\tilde{g}} + m_t)^2 - m_{\tilde{t}_1}^2)(\cos\theta - \sin\theta) \right. \\ & \left. - f_2((m_{\tilde{g}} - m_t)^2 - m_{\tilde{t}_1}^2)(\sin\theta + \cos\theta) \right), \end{aligned} \quad (3)$$

where

$$f_1 = f_1^c + f_1^d, \quad f_2 = f_2^c + f_2^d, \quad (4)$$

where f_i^c are the contributions in the form of counterterms,

$$\begin{aligned}
f_1^c &= \sqrt{2}(f_L \cos \theta - f_R \sin \theta), \\
f_2^c &= \sqrt{2}(-f_L \cos \theta - f_R \sin \theta), \\
f_L &= \frac{1}{2}Z_L^t + \frac{1}{2}Z_R^{\tilde{g}} + \delta g_s/g_s - \tan \theta \delta \theta + \frac{1}{2}Z_{\tilde{t}_1}, \\
f_R &= \frac{1}{2}Z_R^t + \frac{1}{2}Z_L^{\tilde{g}} + \delta g_s/g_s + \cot \theta \delta \theta + \frac{1}{2}Z_{\tilde{t}_1}.
\end{aligned} \tag{5}$$

The renormalization constants in Eq. 5 are,

$$\begin{aligned}
Z_L^t &= \frac{1}{12\pi^2 m_t^2} \left(\sin \theta^2 (m_{\tilde{t}_1}^2 - m_{\tilde{g}}^2) B_0(0, m_{\tilde{g}}^2, m_{\tilde{t}_1}^2) + \cos \theta^2 (m_{\tilde{t}_2}^2 - m_{\tilde{g}}^2) B_0(0, m_{\tilde{g}}^2, m_{\tilde{t}_2}^2) \right. \\
&\quad - m_t^2 B_0(0, \lambda^2, m_t^2) + \left(\sin \theta^2 (m_{\tilde{g}}^2 - m_{\tilde{t}_1}^2) - \cos \theta^2 m_t^2 \right) B_0(m_t^2, m_{\tilde{g}}^2, m_{\tilde{t}_1}^2) \\
&\quad + \left(\cos \theta^2 (m_{\tilde{g}}^2 - m_{\tilde{t}_2}^2) - \sin \theta^2 m_t^2 \right) B_0(m_t^2, m_{\tilde{g}}^2, m_{\tilde{t}_2}^2) \\
&\quad + m_t^2 (-m_{\tilde{g}}^2 + m_{\tilde{t}_1}^2 - m_t^2 + 2m_{\tilde{g}} m_t \sin(2\theta)) \dot{B}(m_t^2, m_{\tilde{g}}^2, m_{\tilde{t}_1}^2) \\
&\quad + m_t^2 (-m_{\tilde{g}}^2 + m_{\tilde{t}_2}^2 - m_t^2 - 2m_{\tilde{g}} m_t \sin(2\theta)) \dot{B}(m_t^2, m_{\tilde{g}}^2, m_{\tilde{t}_2}^2) \\
&\quad \left. + 4m_t^4 \dot{B}(m_t^2, \lambda^2, m_t^2) \right), \\
Z_R^t &= Z_L^t(\theta \rightarrow \pi/2 - \theta), \\
Z_L^{\tilde{g}} &= \frac{1}{32\pi^2 m_{\tilde{g}}^2} \left(\sum_{\tilde{q}} \{ m_{\tilde{q}_L}^2 B_0(0, m_q^2, m_{\tilde{q}_L}^2) + m_{\tilde{q}_R}^2 B_0(0, m_q^2, m_{\tilde{q}_R}^2) \right. \\
&\quad - (m_{\tilde{g}}^2 + m_{\tilde{q}_L}^2) B_0(m_{\tilde{g}}^2, m_q^2, m_{\tilde{q}_L}^2) - (m_{\tilde{g}}^2 + m_{\tilde{q}_R}^2) B_0(m_{\tilde{g}}^2, m_q^2, m_{\tilde{q}_R}^2) \\
&\quad + 2m_{\tilde{g}}^2 (m_{\tilde{q}_L}^2 - m_{\tilde{g}}^2) \dot{B}(m_{\tilde{g}}^2, m_q^2, m_{\tilde{q}_L}^2) + 2m_{\tilde{g}}^2 (m_{\tilde{q}_R}^2 - m_{\tilde{g}}^2) \dot{B}(m_{\tilde{g}}^2, m_q^2, m_{\tilde{q}_R}^2) \} \\
&\quad + (m_{\tilde{t}_1}^2 - m_t^2) B_0(0, m_t^2, m_{\tilde{t}_1}^2) + (m_{\tilde{t}_2}^2 - m_t^2) B_0(0, m_t^2, m_{\tilde{t}_2}^2) \\
&\quad - (m_{\tilde{g}}^2 + m_{\tilde{t}_1}^2 - m_t^2) B_0(m_{\tilde{g}}^2, m_t^2, m_{\tilde{t}_1}^2) - (m_{\tilde{g}}^2 + m_{\tilde{t}_2}^2 - m_t^2) B_0(m_{\tilde{g}}^2, m_t^2, m_{\tilde{t}_2}^2) \\
&\quad + 2m_{\tilde{g}}^2 (m_{\tilde{t}_1}^2 - m_{\tilde{g}}^2 - m_t^2 + 2m_{\tilde{g}} m_t \sin(2\theta)) \dot{B}(m_{\tilde{g}}^2, m_t^2, m_{\tilde{t}_1}^2) \\
&\quad + 2m_{\tilde{g}}^2 (m_{\tilde{t}_2}^2 - m_{\tilde{g}}^2 - m_t^2 - 2m_{\tilde{g}} m_t \sin(2\theta)) \dot{B}(m_{\tilde{g}}^2, m_t^2, m_{\tilde{t}_2}^2) \\
&\quad \left. - 6m_{\tilde{g}}^2 B_0(0, m_{\tilde{g}}^2, \lambda^2) + 24m_{\tilde{g}}^4 \dot{B}(m_{\tilde{g}}^2, m_{\tilde{g}}^2, \lambda^2) \right), \\
Z_R^{\tilde{g}} &= Z_L^{\tilde{g}}, \\
Z_{\tilde{t}_1} &= \frac{1}{6\pi^2} \left(-B_0(m_{\tilde{t}_1}^2, m_{\tilde{g}}^2, m_t^2) + B_0(m_{\tilde{t}_1}^2, \lambda^2, m_{\tilde{t}_1}^2) \right. \\
&\quad + (m_{\tilde{g}}^2 - m_{\tilde{t}_1}^2 + m_t^2) \dot{B}(m_{\tilde{t}_1}^2, m_{\tilde{g}}^2, m_t^2) + 2m_{\tilde{t}_1}^2 \dot{B}(m_{\tilde{t}_1}^2, \lambda^2, m_{\tilde{t}_1}^2) \\
&\quad \left. - 2m_{\tilde{g}} m_t \sin(2\theta) \dot{B}(m_{\tilde{t}_1}^2, m_{\tilde{g}}^2, m_t^2) \right). \tag{6}
\end{aligned}$$

We found the on mass shell definition for the counterterm of stops mixing,

$$\begin{aligned}
\delta\theta &= \frac{1}{2}(\delta Z^{12} + \delta Z^{21}) = \frac{1}{2} \frac{\sum^{\tilde{t}_1\tilde{t}_2}(m_{\tilde{t}_2}^2) - \sum^{\tilde{t}_1\tilde{t}_2}(m_{\tilde{t}_1}^2)}{m_{\tilde{t}_2}^2 - m_{\tilde{t}_1}^2} \\
&= \frac{m_t m_{\tilde{g}} \cos(2\theta)}{6\pi^2(m_{\tilde{t}_2}^2 - m_{\tilde{t}_1}^2)} \left((B_0(m_{\tilde{t}_2}^2, m_{\tilde{g}}^2, m_t^2) - B_0(m_{\tilde{t}_1}^2, m_{\tilde{g}}^2, m_t^2)) \right)
\end{aligned} \tag{7}$$

is properiate for our calculation, which has been adopted in [15]. The counterterm of the $SU(3)_c$ coupling is [11],

$$\delta g_s/g_s = -\frac{3\alpha_s}{2}\Delta. \tag{8}$$

The f_i^d in Eq. 4 are the contributions from the 3-points diagrams,

$$\begin{aligned}
f_1^d &= \frac{\cos\theta - \sin\theta}{96\sqrt{2}\pi^2} \left((9 - \sin(2\theta))B_0(m_t^2, m_{\tilde{g}}^2, m_{\tilde{t}_1}^2) + \sin(2\theta)B_0(m_t^2, m_{\tilde{g}}^2, m_{\tilde{t}_2}^2) \right. \\
&\quad + 35B_0(m_t^2, \lambda^2, m_t^2) + 18m_{\tilde{g}}(3m_{\tilde{g}} + m_t)C_0^{(1)} - 18(m_t^2 - m_{\tilde{t}_1}^2 - m_{\tilde{g}}^2)C_0^{(2)} \\
&\quad + (-m_t^2 - m_{\tilde{t}_1}^2 + m_{\tilde{g}}^2)C_0^{(3)} - 2m_t^2 \sin(2\theta)C_0^{(4)} + 2m_t(-m_{\tilde{g}} + m_t + m_t \sin(2\theta))C_0^{(5)} \\
&\quad + 18(-2k_1 \cdot p + 3m_{\tilde{g}}^2 + m_{\tilde{g}}m_t)C_1^{(1)} + 18(-2k_1 \cdot p + 2m_{\tilde{g}}^2 + m_{\tilde{g}}m_t)C_1^{(2)} - 2m_{\tilde{g}}m_tC_1^{(3)} \\
&\quad - 2m_{\tilde{g}}(m_{\tilde{g}} + (m_{\tilde{g}} - m_t) \sin(2\theta))C_1^{(4)} - 2m_{\tilde{g}}(m_t + (m_t - m_{\tilde{g}}) \sin(2\theta))C_1^{(5)} \\
&\quad + 18(-4k_1 \cdot p + 3m_{\tilde{g}}^2 + m_t^2)C_2^{(1)} + 18(-3k_1 \cdot p + 2m_{\tilde{g}}^2 + m_t^2)C_2^{(2)} - 2(k_1 \cdot p - m_t^2)C_2^{(3)} \\
&\quad - 2(m_{\tilde{g}}^2 - m_{\tilde{g}}m_t + (-k_1 \cdot p + m_{\tilde{g}}^2 - m_{\tilde{g}}m_t + m_t^2) \sin(2\theta))C_2^{(4)} \\
&\quad \left. - 2(-m_t^2 + m_{\tilde{g}}m_t + (k_1 \cdot p - m_{\tilde{g}}^2 + m_{\tilde{g}}m_t - m_t^2) \sin(2\theta))C_2^{(5)} \right), \\
f_2^d &= \frac{\cos\theta + \sin\theta}{96\sqrt{2}\pi^2} \left(-(9 + \sin(2\theta))B_0(m_t^2, m_{\tilde{g}}^2, m_{\tilde{t}_1}^2) + \sin(2\theta)B_0(m_t^2, m_{\tilde{g}}^2, m_{\tilde{t}_2}^2) \right. \\
&\quad - 35B_0(m_t^2, \lambda^2, m_t^2) + 18m_{\tilde{g}}(-3m_{\tilde{g}} + m_t)C_0^{(1)} + 18(m_t^2 - m_{\tilde{t}_1}^2 - m_{\tilde{g}}^2)C_0^{(2)} \\
&\quad - (-m_t^2 - m_{\tilde{t}_1}^2 + m_{\tilde{g}}^2)C_0^{(3)} - 2m_t^2 \sin(2\theta)C_0^{(4)} + 2m_t(-m_{\tilde{g}} - m_t + m_t \sin(2\theta))C_0^{(5)} \\
&\quad + 18(2k_1 \cdot p - 3m_{\tilde{g}}^2 + m_{\tilde{g}}m_t)C_1^{(1)} + 18(2k_1 \cdot p - 2m_{\tilde{g}}^2 + m_{\tilde{g}}m_t)C_1^{(2)} - 2m_{\tilde{g}}m_tC_1^{(3)} \\
&\quad + 2m_{\tilde{g}}(m_{\tilde{g}} - (m_{\tilde{g}} + m_t) \sin(2\theta))C_1^{(4)} + 2m_{\tilde{g}}(-m_t + (m_t + m_{\tilde{g}}) \sin(2\theta))C_1^{(5)} \\
&\quad - 18(-4k_1 \cdot p + 3m_{\tilde{g}}^2 + m_t^2)C_2^{(1)} - 18(-3k_1 \cdot p + 2m_{\tilde{g}}^2 + m_t^2)C_2^{(2)} + 2(k_1 \cdot p - m_t^2)C_2^{(3)} \\
&\quad + 2(m_{\tilde{g}}^2 + m_{\tilde{g}}m_t + (k_1 \cdot p - m_{\tilde{g}}^2 - m_{\tilde{g}}m_t - m_t^2) \sin(2\theta))C_2^{(4)} \\
&\quad \left. + 2(-m_t^2 - m_{\tilde{g}}m_t + (-k_1 \cdot p + m_{\tilde{g}}^2 + m_{\tilde{g}}m_t + m_t^2) \sin(2\theta))C_2^{(5)} \right). \tag{9}
\end{aligned}$$

In the presentaion of the formulas above, we have used notations,

$$\Delta = \frac{2}{4 - D} - \gamma_E + \ln(4\pi),$$

$$k_1.p = \frac{m_t^2 - m_{\tilde{t}_1}^2 + m_{\tilde{g}}^2}{2},$$

$$\dot{B}(p^2, m_a^2, m_b^2) = \partial B_0(p^2, m_a^2, m_b^2) / \partial p^2, \quad (10)$$

the definitions of the scalar integrals Bs and Cs could be found in Ref. [13,16], and the indexes (1) – (5) of C functions have the variables

$$(m_{\tilde{g}}^2, m_t^2, m_{\tilde{t}_1}^2, m_{\tilde{g}}^2, \lambda^2, m_t^2), (m_{\tilde{g}}^2, m_t^2, m_{\tilde{t}_1}^2, \lambda^2, m_{\tilde{g}}^2, m_{\tilde{t}_1}^2), (m_{\tilde{g}}^2, m_t^2, m_{\tilde{t}_1}^2, m_{\tilde{t}_1}^2, m_t^2, \lambda^2),$$

$$(m_{\tilde{g}}^2, m_t^2, m_{\tilde{t}_1}^2, m_t^2, m_{\tilde{t}_1}^2, m_{\tilde{g}}^2), (m_{\tilde{g}}^2, m_t^2, m_{\tilde{t}_1}^2, m_t^2, m_{\tilde{t}_2}^2, m_{\tilde{g}}^2),$$

respectively.

B. Real corrections

The infrad divergence arised from the virtual massless gluon corrections are compensated by the real bremsstrahlung corrections, i.e. the three-body decay

$$t(p) \rightarrow \tilde{g}(k_1)\tilde{t}_1(k_2)g(k). \quad (11)$$

The corresponding matrix element as given by the Feynman diagrams (Fig. 1 (f)) is

$$M_b = 4\sqrt{2}\pi\alpha_s\bar{U}(k1)\{-i f_{abc}T_c \frac{1}{2k.k_1}\not{(\not{k} + \not{k}_1 + m_{\tilde{g}})}(\sin\theta P_R - \cos\theta P_L)$$

$$+ T_b T_a \frac{1}{-2p.k}(\sin\theta P_R - \cos\theta P_L)(\not{k}_1 + \not{k}_2 + m_t)\not{(\not{k}_1 + \not{k}_2 + m_t)}$$

$$+ T_a T_b \frac{1}{2k_2.k}(\sin\theta P_R - \cos\theta P_L)(2k_2 + k).\epsilon\}U(p), \quad (12)$$

where ϵ denotes the polarization vector of gluon. Squaring the matrix element, performing the polarization and color sum over the square of the amplitude and integrating over the phase space yields the complete bremsstrahlung cross section as

$$\Gamma_b = \frac{\alpha_s^2}{24\pi m_t}\{48[2m_{\tilde{g}}^2(m_{\tilde{g}}^2 - m_{\tilde{t}_1}^2 + m_t^2 - 2m_{\tilde{g}}m_t \sin(2\theta))I_{11} + 2m_{\tilde{g}}^2I_1 + I_1^0$$

$$- 2m_{\tilde{g}}m_t \sin(2\theta)I_1] + \frac{64}{3}[2m_t^2(-m_{\tilde{g}}^2 + m_{\tilde{t}_1}^2 - m_t^2 + 2m_{\tilde{g}}m_t \sin(2\theta))I_{00}$$

$$- 2m_t^2I_0 - I_0^1 + 2m_{\tilde{g}}m_t \sin(2\theta)I_0] + \frac{64}{3}[2m_{\tilde{t}_1}^2(-m_{\tilde{g}}^2 + m_{\tilde{t}_1}^2 - m_t^2$$

$$+ 2m_{\tilde{g}}m_t \sin(2\theta))I_{22} + (-m_{\tilde{g}}^2 + 3m_{\tilde{t}_1}^2 - m_t^2 + 2m_{\tilde{g}}m_t \sin(2\theta))I_2 + I]\}$$

$$\begin{aligned}
& + \frac{8}{3} \left[-(2m_{\tilde{g}}^4 - 4m_{\tilde{g}}^2 m_{\tilde{t}_1}^2 + 2m_{\tilde{t}_1}^4 - 2m_t^4 - 4m_{\tilde{g}} m_t \sin(2\theta)(m_{\tilde{g}}^2 - m_{\tilde{t}_1}^2 - m_t^2)) I_{02} \right. \\
& \left. + (m_{\tilde{g}}^2 + m_{\tilde{t}_1}^2 + m_t^2) I_2 + 2(m_{\tilde{t}_1}^2 - m_{\tilde{g}}^2) I_0 + I - 2m_{\tilde{g}} m_t \sin(2\theta)(I_2 - I_0) \right] \\
& + 24 \left[-2(m_{\tilde{g}}^2 - m_{\tilde{t}_1}^2 + m_t^2)^2 - 2m_{\tilde{g}} m_t \sin(2\theta)(m_{\tilde{g}}^2 - m_{\tilde{t}_1}^2 + m_t^2) I_{01} \right. \\
& \left. + 2(m_t^2 - m_{\tilde{g}}^2) I_0 + 2(m_{\tilde{t}_1}^2 - m_t^2 + m_{\tilde{g}} m_t \sin(2\theta))(I_1 + I_0) - 2I \right] \\
& + 24 \left[2(-m_{\tilde{g}}^4 + (m_{\tilde{t}_1}^4 - 2m_{\tilde{t}_1}^2 m_t^2 + m_t^4 + 2m_{\tilde{g}} m_t \sin(2\theta)(m_{\tilde{g}}^2 + m_{\tilde{t}_1}^2 - m_t^2)) I_{12} \right. \\
& \left. - (m_{\tilde{g}}^2 + m_{\tilde{t}_1}^2 + m_t^2) I_2 + 2(m_{\tilde{t}_1}^2 - m_t^2) I_1 - I \right]. \tag{13}
\end{aligned}$$

Here the hard gluon has been included and the definition of function $I_{ab\dots}^{AB\dots}$ are

$$I_{ab\dots}^{AB\dots} = \frac{1}{\pi^2} \int \frac{d^3 k_1}{2k_1^0} \frac{d^3 k_2}{2k_2^0} \frac{d^3 k}{2k^0} \delta^4(p - k_1 - k_2 - k) \frac{(\pm k.p_A)(\pm k.P_B)\dots}{(\pm k.p_a)(\pm k.P_b)\dots}, \tag{14}$$

where the minus corresponds top quark and plus corresponds gluino and stop*.

III. NUMERICAL RESULTS

In the MSSM the mass eigenstates \tilde{q}_1 and \tilde{q}_2 of the squarks are related to the interaction eigenstates \tilde{q}_L and \tilde{q}_R by [17]

$$\begin{pmatrix} \tilde{q}_1 \\ \tilde{q}_2 \end{pmatrix} = R^{\tilde{q}} \begin{pmatrix} \tilde{q}_L \\ \tilde{q}_R \end{pmatrix} \quad \text{with} \quad R^{\tilde{q}} = \begin{pmatrix} \cos \theta_{\tilde{q}} & \sin \theta_{\tilde{q}} \\ -\sin \theta_{\tilde{q}} & \cos \theta_{\tilde{q}} \end{pmatrix}. \tag{15}$$

Following the notation of [17], the mixing angle $\theta_{\tilde{q}}$ and the masses $m_{\tilde{q}_{1,2}}$ can be calculated by diagonalizing the following mass matrices

$$\begin{aligned}
M_{\tilde{q}}^2 &= \begin{pmatrix} M_{LL}^2 & M_{LR}^2 \\ M_{RL}^2 & M_{RR}^2 \end{pmatrix}, \\
M_{LL}^2 &= m_{\tilde{Q}}^2 + m_q^2 + m_z^2 \cos 2\beta (I_q^{3L} - e_q \sin^2 \theta_w), \\
M_{RR}^2 &= m_{\tilde{U}, \tilde{D}}^2 + m_q^2 + m_z^2 \cos 2\beta e_q \sin^2 \theta_w. \tag{16}
\end{aligned}$$

* It should be noticed that (D.11) and (D.12) in Ref. [13] must be corrected as following: the first term in the square bracket of (D.11) must be replaced by the corresponding term in (D.12), and *vice versa*

From Eqs. 15 and 16, $m_{\tilde{t}_{1,2}}$ and θ can be derived as

$$\begin{aligned} m_{\tilde{t}_{1,2}}^2 &= \frac{1}{2} \left[M_{LL}^2 + M_{RR}^2 \mp \sqrt{(M_{LL}^2 - M_{RR}^2)^2 + 4M_{LR}^4} \right] \\ \tan \theta &= \frac{m_{\tilde{t}_1}^2 - M_{LL}^2}{M_{LR}^2}. \end{aligned} \quad (17)$$

For the numerical calculations, we choose $m_t = 176.0$ GeV and $\alpha_S = 0.118$, and always assume that the soft SUSY breaking mass terms $m_{\tilde{U}} = m_{\tilde{D}} = m_{\tilde{Q}} = m_S$. For simplicity, we also define a variable $r = M_{LL}^2/M_{LR}^2$.

In Fig. 2, we show the decay widths and the QCD relative corrections as function of $m_{\tilde{t}_1}$, assuming $r = 0.9$. The definition of relative correction is $\delta = \Gamma_1/\Gamma_0$. From these curves, we can see that the decay widths, which are not sensitive to the light gluino mass allowed by experiments, decrease with the increment of $m_{\tilde{t}_1}$, which is the nature consequence of the shrink of the phase space, and the decay width could be comparable with the $t \rightarrow bW^+$ channel in a large range of parameter space provided that this decay process is allowed kinetically. On the other hand, the QCD corrections always enhanced the decay widths, for $m_{\tilde{t}_1} = 160$ GeV, the corrections exceed 40%.

In Fig. 3, we show the same results, but changing the way of varying the mass of the lighter stop, i.e., varying r while fixed soft SUSY breaking mass term m_S as 300 GeV. We can see these results are very close to Fig. 2, which is due to the fact that the contributions from other squarks (relatively heavy) are less important.

To summarize, we have calculated the decay width of the process $t \rightarrow \tilde{g}\tilde{t}_1$ including the one loop QCD corrections. From our numerical examples, we can see that the QCD corrections could enhance the decay widths over 10% in a very large mass range of the lighter stop, and the decay widths of the process could be larger than that of the channel $t \rightarrow bW^+$. Our results show that this process, if allowed kinetically, must have very important phenomenology consequences; at least, new constrains for the masses of the lighter stop and gluino can be obtained.

[1] J. Ellis and S. Rudaz, Phys.Lett **B128**,248 (1983).

[2] $D\emptyset$, EPS-HEP Conf., Jerusalem (1997) Ref.102; CDF, Phys. Rev. D 56, R1357 (1997), Phys. Rev. Lett. 75,618 (1995) and Phys. Rev. Lett. 69, 3439 (1992); UA2, Phys.Lett B. 235, 363(1990); UA1, Phys. Lett. B 198, 261 (1987).

[3] Aleph Collaboration, R.Barate et al., Z.Phys.C 76, 1 (1997); F.Csikor and Z.Fordor, Phys. Rev. Lett. 78, 4335 (1997); hep-ph/9712269.

[4] S. Dawson, Nucl. Phys. **B261**, 297 (1985); H. Dreiner, hep-ph/9707435; L. Clavelli and I. Terekhov, Phys. Lett. **B429**, 51 (1998).

[5] G. Bhattacharyya, Nucl. Phys. Proc. Suppl. **A52**, 83 (1997); G.R.Farrar, Nucl.Phys. **B** (Proc.Suppl) 62 (1998) 485.

[6] F. E. Close, G. R. Farrar, and Z. P. Li. Phys. Rev. D55, 5749 (1997).

[7] CDF Collaboration, Phys. Rev. Lett. **77**, 438 (1996).

[8] F.Abe et al, Phys.Rev.Lett. 73,225 (1994),Phys.Rev.Lett.74, 2626(1995); S. Abachi et al, Phys.Rev.Lett. 74, 2632 (1995).

[9] Report of the Top Physics working group at the 1996 DPF/DPB Snowmass workshop, hep-ph/9704243; P.C. Bhat, H.Prosper, S.S. Snyder, hep-ex/9809011;

[10] C.S. Li, P. Nadolsky and C.P. Yuan, Phys.Rev. **D58**, 095004 (1998); L. Clavelli and G.R. Goldstein, Phys.Rev. **D58**, 095012 (1998); I. Terekhov, Phys.Lett. **B412**, 86 (1997).

[11] W. Beenakker, R. Hopker, T. Plehn and P. Zerwas, Z. Phys. **C95**, 349 (1997).

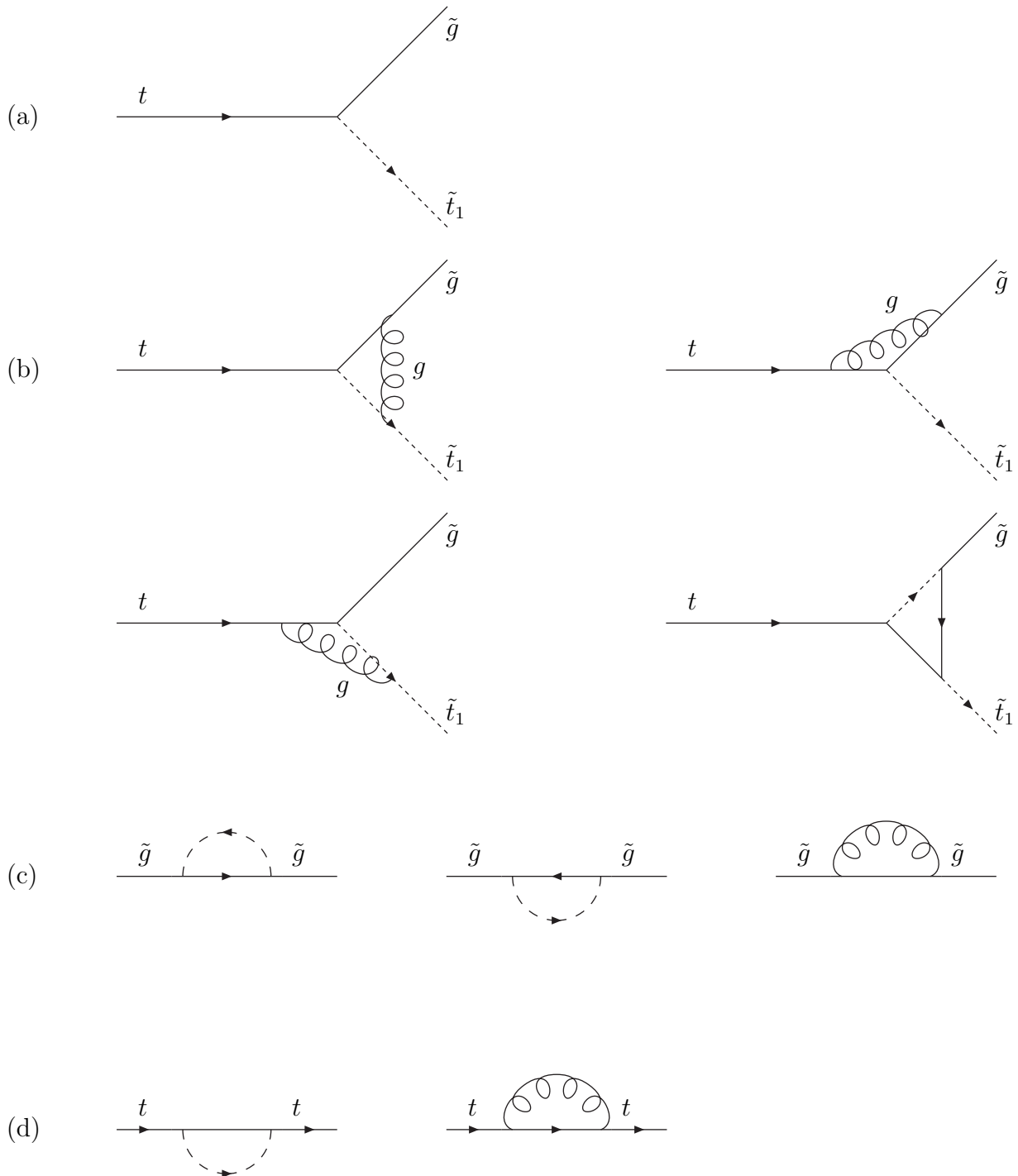
[12] W.Siegel, Phys.Lett. B84 193(1979); D.M.Capper, D.R.T.Jones and P.Van Nieuwenhuizen, Nucl.Phys.B167, 479 (1980).

[13] A. Denner, Fortschr. Phys. 41, 307 (1993).

[14] S. Sirlin, Phys. Rev. **D22**, 971 (1980); W. J. Marciano and A. Sirlin, ibid. 22, 2695 (1980); 31, 213(E) (1985); A. Sirlin and W.J. Marciano, Nucl. Phys. B 189, 442 (1981); K.I. Aoki et.al.,

Prog. Theor. Phys. Suppl. 73, 1 (1982).

- [15] H.Eberl,A.Bartl and W.Majerotto, Nucl. Phys.B472, 481 (1996); J. Guasch, J. Sola and W. Hollik, hep-ph/9802329.
- [16] G. Passarino and M. Veltman, Nucl. Phys. B 33, 151 (1979); R. Mertig, M. Bohm and A. Denner, Comp. Phys. Comm. 64, 345 (1991).
- [17] H.E. Haber and G.L. Kane, Phys.Rep. **117**, 75 (1985); J.F. Gunion and H.E. Haber, Nucl. Phys. **B272**, 1(1986); For a review see, e.g. J.F. Gunion et. al., Higgs Hunter's Guide (Addison-Wesley, Reading, MA,1990).



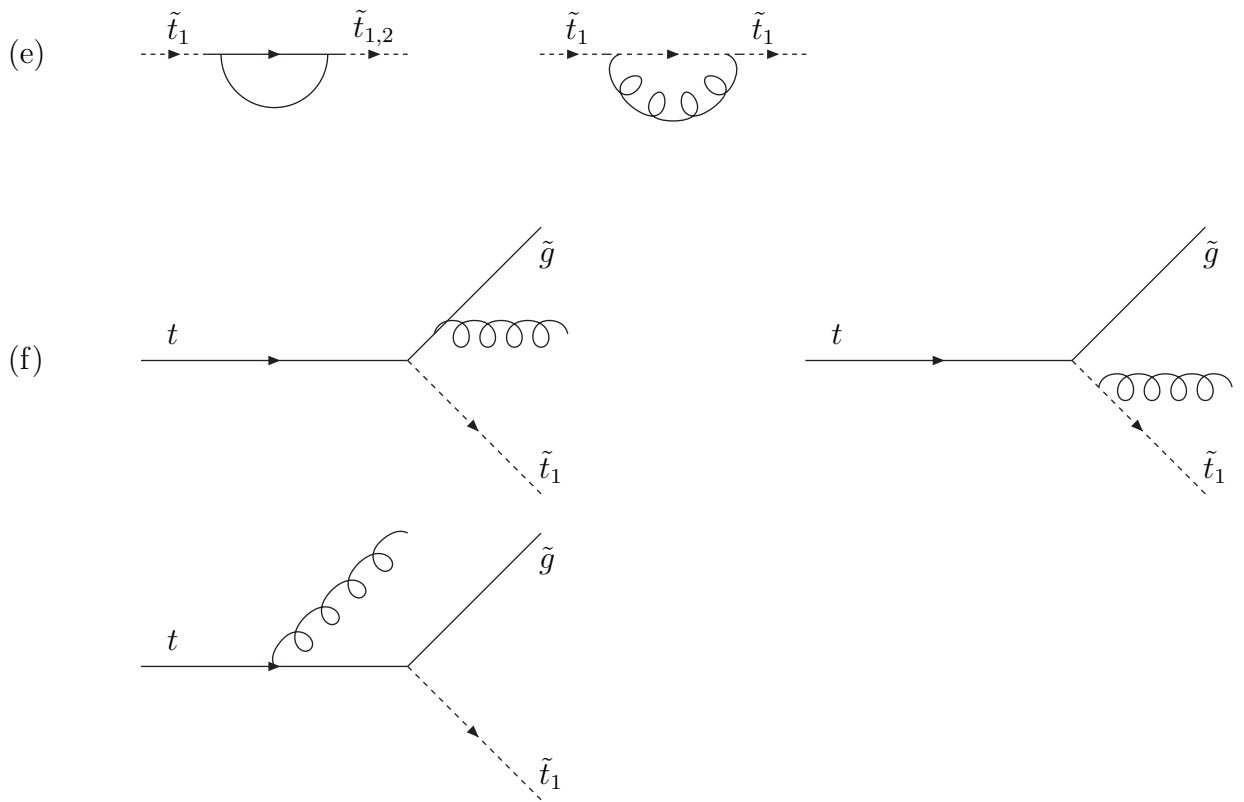


FIG. 1. Feynman diagrams for the process $t \rightarrow \tilde{g}\tilde{t}_1$.

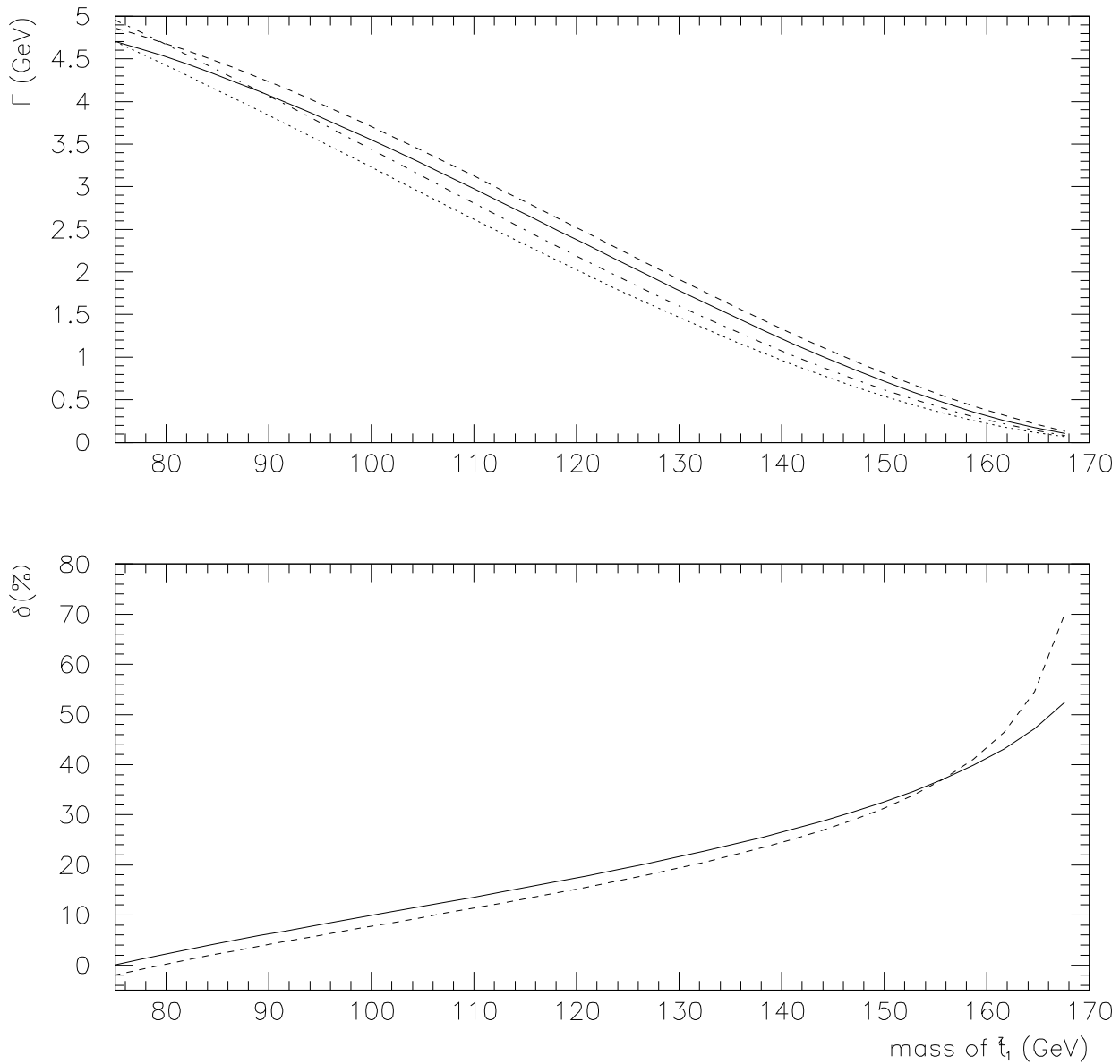


FIG. 2. Decay widths and relative corrections as function of $m_{\tilde{t}_1}$, where $r = 0.9$ and the lighter stop mass is adjusted by varying the soft SUSY breaking mass term m_S . For above figure, the solid and dashed lines represent the decay widths including QCD corrections for $m_{\tilde{g}} = 1$ and 5 GeV, and the dotted and dot-dashed lines represent the tree level decay widths for $m_{\tilde{g}} = 1$ and 5 GeV, respectively. For below figure, the solid and dashed lines represent the relative corrections for $m_{\tilde{g}} = 1$ and 5 GeV, respectively.

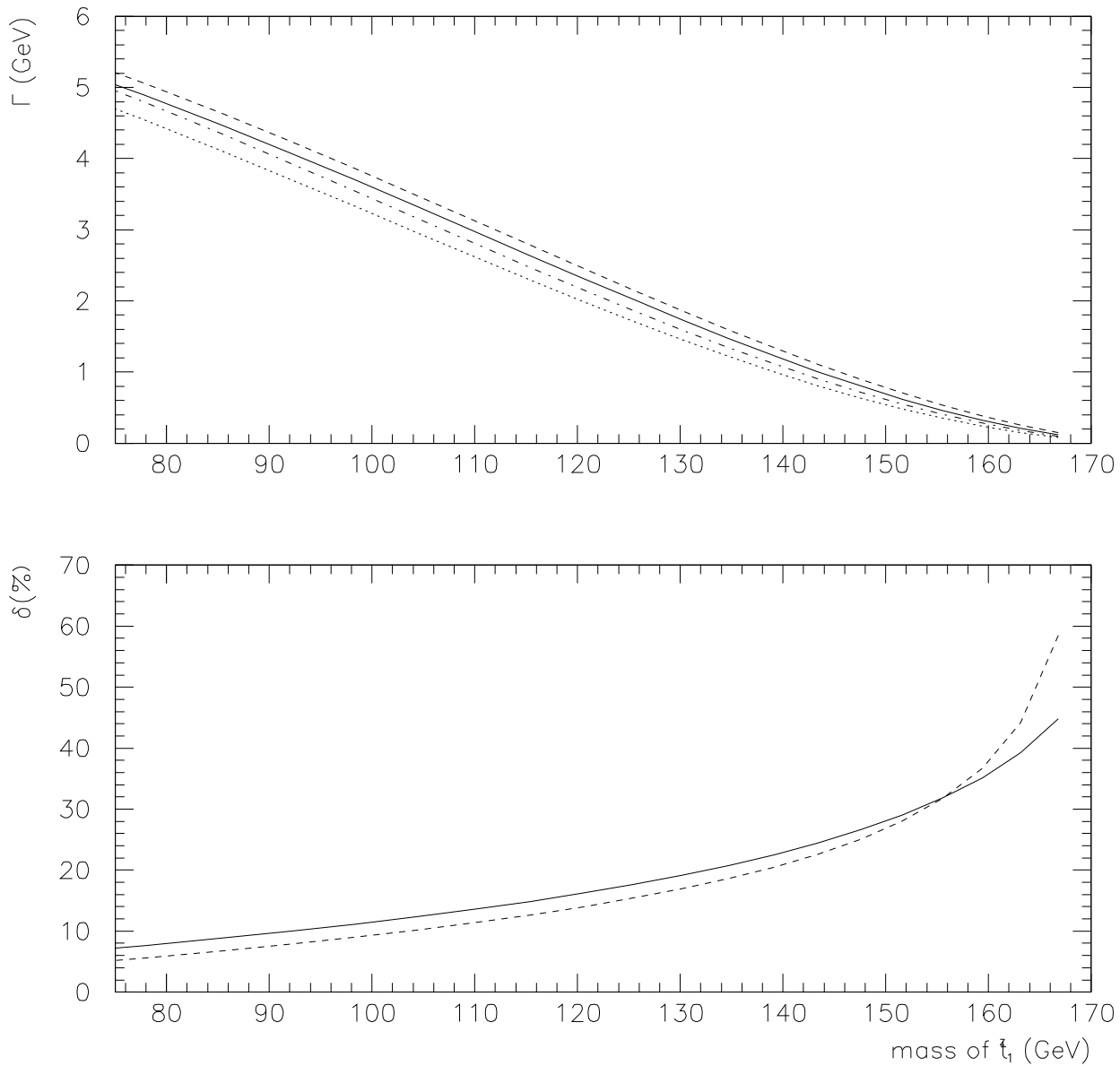


FIG. 3. Same with Fig. 2 but fixed the soft SUSY breaking mass term m_S as 300 GeV and the lighter stop mass is adjusted by varying r .